

The effect of lattice strain on catalytic activity

Westsson, Emma; Picken, Stephen; Koper, Ger

DOI

[10.1039/c8cc09063g](https://doi.org/10.1039/c8cc09063g)

Publication date

2019

Document Version

Final published version

Published in

Chemical Communications

Citation (APA)

Westsson, E., Picken, S., & Koper, G. (2019). The effect of lattice strain on catalytic activity. *Chemical Communications*, 55(9), 1338-1341. <https://doi.org/10.1039/c8cc09063g>

Important note

To cite this publication, please use the final published version (if applicable). Please check the document version above.

Copyright

Other than for strictly personal use, it is not permitted to download, forward or distribute the text or part of it, without the consent of the author(s) and/or copyright holder(s), unless the work is under an open content license such as Creative Commons.

Takedown policy

Please contact us and provide details if you believe this document breaches copyrights. We will remove access to the work immediately and investigate your claim.



The effect of lattice strain on catalytic activity†

 Emma Westsson,  Stephen Picken  and Ger Koper *

 Cite this: *Chem. Commun.*, 2019, 55, 1338

 Received 14th November 2018,
Accepted 7th December 2018

DOI: 10.1039/c8cc09063g

rsc.li/chemcomm

We report on the effect of lattice strain in three different types of core–shell electrocatalyst particles on their catalytic activity towards the oxygen reduction reaction. We decouple the changes in catalytic activity with respect to a geometrical and an energetic contribution, both of electronic origin.

The use of core–shell particles as catalysts, such as for fuel cells, entails a number of benefits. Firstly, it opens up the possibility to assess the properties of individual layers as well as to manipulate their structure. Secondly, core–shell particles as opposed to pure particles offer a more efficient material usage. Finally, it offers opportunities to use the core material properties for manipulation and handling of the particles.¹ For core–shell particles a gain in mass activity is to be expected to scale with shell thickness, *e.g.* roughly 10% increase in mass activity for a 20% reduction of shell content in favour of core content. However, as demonstrated here other factors play a more important role. The motivation for our research is to explore how the catalytic properties of the core–shell surface can be enhanced by manipulating its physical properties.

Fitting a thin layer of platinum onto another metal is bound to have consequences for the electronic properties of the Pt shell, both geometrically through lattice mismatch and electronically through shifting of the d-band and, as a consequence, of the binding energies for *e.g.* the oxygen reduction intermediates.^{2–4} Deposited on a metal with a smaller lattice spacing Pt would undergo compressive strain while deposited on a metal with larger lattice spacing, like Au, would result in lattice expansion.⁴ The description of the various strain contributions to XRD response has so far only been fragmental in the literature^{5–7} for which reason a short review is included in the ESI.†

Correlation between surface strain and electro-catalytic activity has been proposed theoretically^{2,3} and demonstrated experimentally.^{6,8} The purpose of this work is to highlight and

contribute to two, previously overlooked, aspects of this phenomenon. Firstly, the multifaceted meaning of “strain” and its impact on XRD reflection analysis and secondly, the correlation between strain and catalytic activity for three different core metals. Here the aim is to build up a volcano-type activity–strain plot through demonstrating that the catalytic activity of platinum is affected positively by lattice compression for Pt@Ni particles and negatively for Pt@Cu and Pt@Fe particles.

All particles for the present study are made using a micro-emulsion as a template in order to obtain monodisperse nanoparticles with a high yield.⁹ In a micro-emulsion the core consisting of Fe, Ni or Cu is synthesized, followed by the addition of a platinum shell through galvanic replacement; see Fig. S1 in the ESI† for a cartoon. Carbon is added as a support to maximize the accessibility of the catalyst particles. The final washing steps in this procedure remove surfactants, retrieve unreacted Pt and ensure that any uncoated cores are washed away leaving intact core–shell particles only.

Size measurements based on Dynamic Light Scattering (DLS) and Transmission Electron Microscopy (TEM) confirm a narrow size distribution and no significant size change between core and core–shell particles, both being 3 ± 0.6 nm, see Table S2 and Fig. S3 (ESI†). An estimate of the final composition of the particles was obtained using Energy Dispersive X-Ray Spectroscopy (EDS) and Inductively Coupled Plasma Atomic Emission Spectroscopy (ICP-AES), see Table S2 (ESI†). Agglomeration of the particles could be identified for samples washed with acid. Due to the small size of the particles and the resolution of TEM no difference in contrast between core and shell was found (see Fig. S4, ESI†).

XRD patterns of Pt@Cu, Pt@Ni, and Pt@Fe samples as well as of pure Pt particles (Fig. S5, ESI†) reveal, as expected, that different core:shell ratios give rise to different amounts of peak shift representing lattice contraction compared to pure Pt particles. The relative lattice shift of the Pt in the core–shell particles with respect to that of pure Pt is interpreted as lattice strain and used to construct the abscissa of Fig. 1. Importantly, one Pt : Me ratio does not give rise to the same strain when the type of core metal is changed.

Technical University of Delft, Maasweg 9, Delft, The Netherlands.

E-mail: g.j.m.koper@tudelft.nl

† Electronic supplementary information (ESI) available. See DOI: 10.1039/c8cc09063g



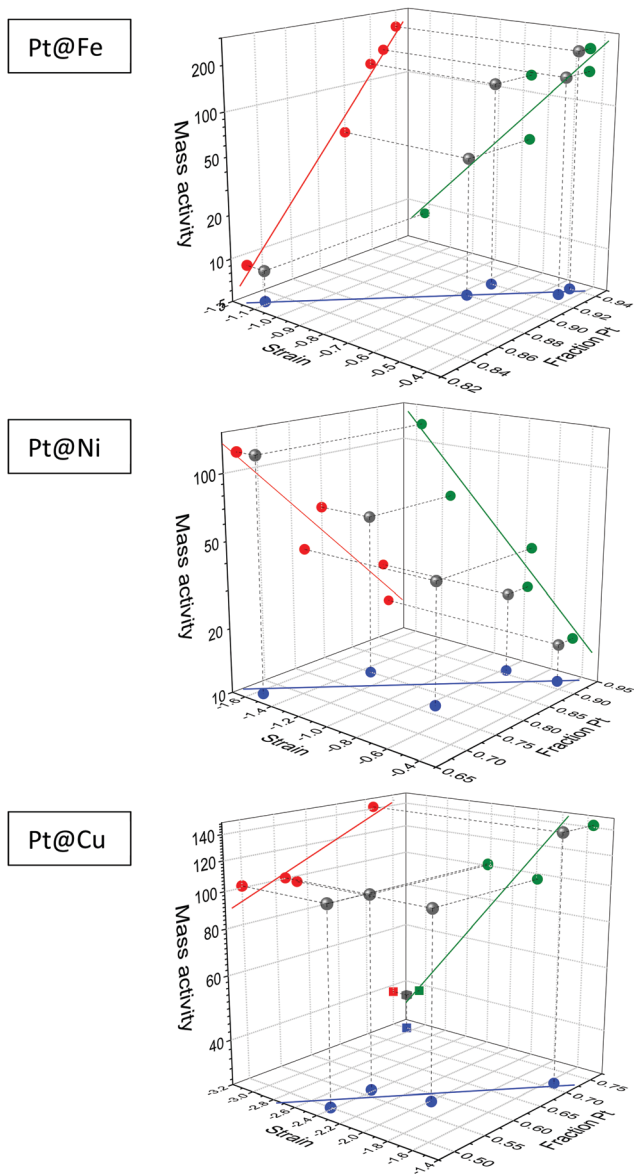


Fig. 1 Pairwise correlations between mass activity ($\text{mA mg}^{-1} \text{Pt}$) and Pt fraction (red), strain (% relative to pure Pt) and mass activity (green), Pt fraction (1 for pure Pt and 0 for pure core metal) and strain (blue) and full correlation (black). Trend lines are discussed in text.

In addition, samples with the most compressed Pt lattice also show the largest peak broadening, *i.e.* Full Width at Half Maximum (FWHM) value (Fig. S6, ESI[†]). The peak broadening increases proportional to the strain. Note that all particles, including pure Pt, have a very similar particle size (Fig. S3, ESI[†]).

Hydrodynamic voltammograms measured in oxygen saturated electrolyte (Fig. S7, ESI[†]) show, despite slight agglomeration, onset potential values above 0.9 V for the oxygen reduction reaction (ORR). Due to non-ideal binding energies of the oxygen reduction intermediates to the Pt surface, there will be an associated overpotential limiting the process from reaching the thermodynamic equilibrium potential of 1.23 V.¹⁰ As a measure of the catalytic activity, the value of the current at 0.8 V was taken representing the region where the electrochemical reduction of

oxygen is kinetically controlled. Interestingly, for the sample with the highest Pt:Fe ratio the kinetic current even outperforms that of pure Pt particles made in micro-emulsion. The mass activity extracted from voltammograms for all particles were used to construct the ordinate in Fig. 1.

A plot of mass activity *versus* lattice strain reveals an exponential dependence where strain influences the activity negatively for Pt@Fe and Pt@Cu and positively for Pt@Ni. For Pt@Fe particles and Pt@Cu particles an increased strain in the Pt lattice seems to decrease the catalytic activity whereas it has an improving effect for Pt@Ni particles, as illustrated in green in Fig. 1. It is clear that the lattice strain is reduced as the Pt fraction in the particle – hence the shell thickness – increases as illustrated in blue in Fig. 1.

The thicker the Pt shell and the less strained the lattice the larger the catalytic activity is for Pt@Fe particles and Pt@Cu particles, illustrated in red in Fig. 1. On the contrary, a thin shell seems beneficial for the activity in Pt@Ni particles. The observation marked as a square in Fig. 1 has been treated as an outlier since its position, even if repeated, deviates considerably from the general trends.

Noteworthy, however, is that the largest strain among all samples prepared was achieved with this composition of Pt and Cu. Mass activity depends exponentially on strain and shell thickness, which is seen by the linear dependency in logarithmic scale in Fig. 1. Strain and shell thickness on the other hand have a linear interdependency.

Let us now first discuss the core-shell nature of the particles on the basis of the following observations: firstly, both metals are present in the particles. Due to the synthesis procedure any uncoated core metal should be washed away. Secondly, the particle surface. Voltammetry shows activity for ORR in the same (or better) range than pure Pt particles made in bi-continuous micro-emulsion.

Furthermore, using micro-emulsions as a template for making nanoparticles generates very similar core-shell particle size distributions independent on metal precursor, as long as the core synthesis is allowed sufficient time. The synthesis procedure can be used for various metal combinations as long as the shell metal has sufficiently higher reduction potential relative to the core metal. The intrinsic particle growth control offered by the micro-emulsion enables a monodispersed sample despite the addition of a Pt shell. This underlines the suitability of using micro-emulsions as template for making core-shell particles. Moreover, a high yield of particles is obtained using this scalable method. Nevertheless, what was learned from the synthesis of one core metal type in terms of reaction parameters could not be used without adaptation to make core-shells with another core metal type. The core-surfactant and shell-surfactant affinity difference is expected to play a major role regarding the extent of galvanic replacement.

The uniformity of the size-distributions allows us to discard specific peak broadening caused by size differences. Nevertheless, all core-shell type samples show peak broadening to a larger extent compared to pure Pt particles of the same particle size. The broadening of the XRD reflections could be caused by the distribution of different interatomic distances in the curved lattice, following the argumentation in the ESI[†] (Fig. S2c). Hence the



FWHM can be used as a rough measure to interpret curvature. Any secondary shoulders due to a “hollow” structure (Fig. S2e, ESI†) are too small to be resolved in our data. It is also crucial to understand whether a hollow sphere acts like a single crystal or like crystal domains. In the case of micro-particles there would most likely be grains making up the shell but for homogeneous nanoparticles the option of having a single domain crystal becomes relevant. If the shell or solid particle is multi-domain then the peak broadening will be more severe than what is predicted in terms of peak broadening due to size. Another situation would be that the crystal is single domain but exhibits internal stresses and strain to some extent.¹¹ Also this can give rise to peak broadening. If the particles were multi-domain, all peaks would most likely be lost since the broadening would flatten out the reflections completely. This is why the most likely scenario here is single crystalline Pt.

Secondly, most particles exhibit a significant shift of the Pt(111), Pt(200) and Pt(220) reflections towards higher 2θ angles compared to the expected positions of Pt and relative to the pure Pt sample, due to the compressive strain arising from Pt being fitted onto a core metal with smaller lattice spacing. Since strain contributes to both peak displacement as well as peak shape it would require extensive analysis to accurately and quantitatively build up a model describing the relation between particle composition and structure to strain.

We have assumed an isostatic pressure on cubic Pt. This might or might not be true in which case the displacement of XRD peaks would not be of equal magnitude amongst the various crystal planes. To the extent of our work we have not seen signs of this.

The Electro-Chemically Active Surface Areas (ECSAs) for some of the catalysts are smaller than expected compared to commercial Pt. It must be remembered though that the calculation of ESCA is based on a number of assumptions well described by Trasatti,¹² including the presence of a fixed density of Pt atoms at the surface ($1.3 \times 10^{15} \text{ cm}^{-2}$) and the completeness of the charge transfer assuming no alterations of the surface. Moreover, the adsorption and desorption of hydrogen is based on bulk Pt. These criteria might very well be compromised in the case of small particles with thin and strained Pt shells. For these reasons activity is expressed in mass activity ($\text{mA mg}^{-1} \text{ Pt}$) rather than specific activity ($\text{mA cm}^{-2} \text{ ECSA}$). One additional factor possibly affecting the surface area negatively is the presence of remaining surfactant on the catalyst surface, although their effect on catalysis has been ambiguously reported.^{9,13,14} On the other hand, agglomeration of particles due to acid washing further keeps the surface area inferior.

Although the catalytic activities exhibited by our core-shell particles are slightly inferior to that of commercial Pt, we see comparable or even a slight improvement in activity compared to pure Pt samples made in bi-continuous micro-emulsion. This is encouraging since there is still some performance to gain through maximizing the particle dispersion on carbon as well as surfactant removal in the synthesis procedure. Moreover, our aim was not to optimize our synthesis but to investigate the effect of strain on the activity.

The catalytic activity of a given metal – in this case Pt – is governed by a set of properties including its local geometric structure and electronic configuration.^{13,15} By creating particles with a core-shell structure it is likely that both these properties are altered, be it negatively or positively. The results in Fig. 1 strengthen the hypothesis of the two contributions: geometrical and energetic, both induced by shell thickness and core material. Furthermore, a change in interatomic distance in the Pt lattice alters the electron band structure and hence, compared to pristine Pt, an alteration in activity due to strain is to be expected. Such correlation has, however, been scarcely investigated due to the complexity of the strain contributions. As “strain” in our activity-strain graph, we have used only the contribution from lattice compression, measured as peak shift, since a fair deconvolution of peak shape is beyond the scope of this paper. However, we have managed to generate core-shell particles with lattice strains ranging from 0.5% up to 3% and showed how the strain affects the ability to catalyse the ORR. For Pt@Fe and Pt@Cu we observe a decrease in activity with lattice strain and the contrary for Pt@Ni.

Since activity is largely controlled by the activation energy it strongly depends on the electronic state of the catalytic substrate.¹⁶ Upon straining the catalyst lattice the activation energy is altered. There is no reason to believe that the unconstrained crystal lattice of the catalyst, Pt in this case, is optimal in activation energy for ORR so that any deviation would only lead to a deterioration. Hence, to a good approximation, we can assume that there is a linear relationship between activation energy and the lattice strain. It can be improved or worsened.

We attempt to decouple the contributions to the activity. On the one hand the contribution from a geometrical perturbation of the lattice, in other words strain, which is measured as peak displacement in XRD. On the other hand the energetic influence from the core metal, which is measured as zero strain catalytic activity. The exponential variation of activity, A , with strain, δ , can be described as: $A = A_0 10^{\alpha \delta}$. A_0 is the activity at zero strain and represents the contribution from the pure metal. α is the linear variation of activation energy with strain (δ). The slope, α , and the intersect at zero strain, A_0 , are shown in Fig. 2 as well as the evidently exponential dependence of activation energy on strain. Furthermore, the Pt@Fe-type particles are the most negatively affected by strain.

The zero-strained activity, A_0 , depicted in orange in Fig. 2 is an extrapolated value since it is impractical to make Pt shells with infinitely little strain. However, the results predict an increase in the catalytic activity for unstrained Pt for Pt@Cu and Pt@Fe. Such lattice would require a surface with curvature of the order of micrometres or more and in that case the benefit of large surface area for the particles would be lost. In this manner we can extrapolate to zero strain, *i.e.* zero geometrical effect, to obtain the pure energetic effect. Nevertheless, the energetic contribution and the geometric contribution to the overall catalytic behaviour of a specific catalyst are closely intertwined – both are consequences of electronic changes. It is however useful to understand the contributions that determine the catalytic behaviour in order to fine-tune it. Our results in Fig. 2 are a gesture to disentangle these effects.



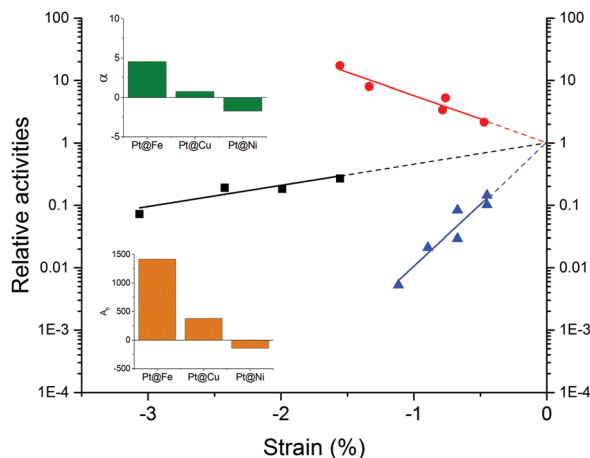


Fig. 2 The effect of strain on the catalytic activity, where Pt@Ni (red), Pt@Cu (black) and Pt@Fe (blue). Relative activity is here defined as A/A_0 , where A_0 is the activity (mA mg^{-1} Pt) extrapolated to zero strain (induced by lattice mismatch). Inset plots show the separation of the metal effect A_0 (orange) and the strain effect (green) on the catalytic activity for Pt coated metal particles.

To summarize, by means of the core-shell particle synthesis described in this paper we were capable to demonstrate that the catalytic activity of the resulting nanoparticles can be tuned by surface strain and core material. We predict the way core-shell particle structure and different types of strain affect the reflections in XRD (ESI[†]).

Combining crystallographic measurements with catalytic activity measurements led us to conclude that the catalytic activity is affected by (at least) two effects: the geometrical effect due to lattice strain as well as the energetic effect on band structure of the shell metal caused by the interplay between the core and shell metal, for which the exact mechanism we leave for theoreticians to study. This is nevertheless a first systematic study of this behaviour.

Yet another result stressing the point that there is more information to gain from XRD analysis, is the dependence of peak broadening on strain. We have shown that, for core-shell particles, the peak broadening in XRD is not only a result of particle size, but also varies systematically with the shell thickness, *i.e.* the strain. Here strain arising from curvature could be the dominating effect, suggestively illustrated by Fig. S2c (ESI[†]).

It becomes evident that Fourier deconvolution of measured peaks, albeit an experimental challenge, becomes an important tool for understanding the real nature of core-shell type particles. The peak shift and broadening, quantifying to a certain extent the lattice strain and curvature respectively, represents the geometric alteration of the Pt lattice. Furthermore, standard electrochemical methods may represent properties of core-shell electro-catalyst particles poorly when operating outside assumptions of standard Pt surfaces.

Manipulating Pt to shift its position in the Volcano plot opens up a new approach in designing catalyst particles. As an extension to this work, other metals than Pt could be studied and possibly take platinum's place as the most active oxygen reduction catalyst.

This work was supported by NanoNextNL. The authors wish to acknowledge Prof. Dr J. J. C. Geerlings, Prof. Dr F. M. Mulder and Ben Norder for discussions and assistance.

Conflicts of interest

There are no conflicts to declare.

Notes and references

- S. Duan and R. Wang, *Mater. Int.*, 2013, **23**, 113–126.
- B. H. J. K. Norskov, *Adv. Catal.*, 2000, **45**, 71–129.
- E. Santos, P. Quaino and W. Schmickler, *Electrochim. Acta*, 2010, **55**, 4346–4352.
- Y. Cai and R. R. Adzic, *Adv. Phys. Chem.*, 2011, **2011**, 1–16.
- B. D. Cullity, *Elements of X-Ray Diffraction*, Addison-Wesley Publishing Company Inc., Massachusetts, 1956.
- Y. Zhang, C. Ma, Y. Zhu, R. Si, Y. Cai, J. X. Wang and R. R. Adzic, *Catal. Today*, 2013, **202**, 50–54.
- P. Bindu and S. Thomas, *J. Theor. Appl. Phys.*, 2014, **8**, 123–134.
- S. E. Temmel, E. Fabbri, D. Pergolesi, T. Lippert and T. J. Schmidt, *ACS Catal.*, 2016, **6**, 7566–7576.
- E. Westsson and G. Koper, *Catalysts*, 2014, **4**, 375–396.
- J. K. Norskov, J. Rossmeisl, A. Logadottir, L. Lindqvist, J. R. Kitchin, T. Bligaard and H. Jonsson, *J. Phys. Chem. B*, 2004, **108**, 17886–17892.
- Y. Zhao and J. Zhang, *J. Appl. Crystallogr.*, 2008, **41**, 1095–1108.
- P. Trasatti, *Pure Appl. Chem.*, 1991, **63**, 711–734.
- M. Shao, *Electrocatalysis in Fuel Cells – A non- and low platinum approach*, Springer, London, 2013.
- J. E. Newton, J. A. Preece, N. V. Rees and S. L. Horswell, *Phys. Chem. Chem. Phys.*, 2014, **16**, 11435–11446.
- A. K. G. Pintu Saji, M. A. Bhat and P. P. Ingole, *ChemPhysChem*, 2016, **17**, 1195–1203.
- E. Roduner, *Chem. Soc. Rev.*, 2014, **43**, 8226–8239.

